

## Energies of quantum QED flux tubes

This article has been downloaded from IOPscience. Please scroll down to see the full text article.

2006 J. Phys. A: Math. Gen. 39 6799

(<http://iopscience.iop.org/0305-4470/39/21/S82>)

View [the table of contents for this issue](#), or go to the [journal homepage](#) for more

### Download details:

IP Address: 171.66.16.105

The article was downloaded on 03/06/2010 at 04:35

Please note that [terms and conditions apply](#).

# Energies of quantum QED flux tubes

**H Weigel**

Fachbereich Physik, Siegen University, Walter Flex Straße 3, 57072 Siegen, Germany

E-mail: [weigel@physik.uni-siegen.de](mailto:weigel@physik.uni-siegen.de)

Received 4 November 2005, in final form 8 January 2006

Published 10 May 2006

Online at [stacks.iop.org/JPhysA/39/6799](http://stacks.iop.org/JPhysA/39/6799)

## Abstract

In this paper, I present recent studies on vacuum polarization energies and energy densities induced by QED flux tubes. I focus on comparing three- and four-dimensional scenarios and the discussion of various approximation schemes in view of the exact treatment.

PACS numbers: 03.65.Nk, 03.70.+k, 04.62.+v

(Some figures in this article are in colour only in the electronic version)

## 1. Introduction and motivation

In this paper, I will present calculations of vacuum polarization energies that we [1] have performed for flux tube configurations in QED. Flux tubes in QED coupled to fermions exhibit interesting phenomena, such as the Aharonov–Bohm effect [2], its consequences for fermion scattering [3], parity anomalies [4], formation of a condensate [5] and exotic quantum numbers [7–9]. Those (non-perturbative) features of the theory that give rise to these unusual phenomena make the analysis more difficult, especially in calculations that require renormalization. The investigation in [10] and the worldline formalism in [11] have addressed some of these issues. Here we provide a comprehensive approach employing techniques from scattering theory to analyse quantum energies of flux tubes.

Our primary motivation for this analysis is to shed light on vortices in more complicated field theories, especially the Z-string in the standard electroweak theory [12]. The Z-string is a vortex configuration carrying magnetic flux in the field of the Z-gauge boson. Since the classical Z-string is known to be unstable [13], the existence of such a vortex would require stabilization via quantum effects [14], perhaps by trapping heavy quarks along the string.

We compare the one-loop energies and energy densities of electromagnetic flux tubes in  $D = 2 + 1$  and  $D = 3 + 1$  spacetime dimensions. The classical calculation is of course the same in the two cases. The quantum corrections to the energy could possibly be very different [11] because of the different divergence structure. In  $D = 3 + 1$ , the bare one-loop energy is divergent and requires renormalization. In  $D = 2 + 1$ , in contrast, the bare energy is finite.

However, a comparison between the two dimensionalities is sensible only when we use the same renormalization conditions, which induces a finite counterterm in the  $D = 2 + 1$  case. Without this finite renormalization, the  $D = 2 + 1$  and  $D = 3 + 1$  energies are qualitatively different.

We also study this problem to analyse several technical puzzles associated with the computation of the one-loop energy of a flux tube. An efficient way to compute the energy is to use scattering data of fermions in the background of the flux tube. However, vortex configurations give long-range potentials, that do not satisfy standard conditions in scattering theory [15], which usually guarantee the analytic properties of scattering data. In turn, these properties are crucial to compute the vacuum polarization energy from scattering data. Hence, we observe subtleties that emerge only because an isolated flux tube is unphysical, and once a region of return flux is included, the scattering problem is well defined. In the limit where the return flux is infinitely spread out, the energy density becomes entirely localized at the original flux tube.

## 2. Theory

We consider the QED Lagrangian

$$\mathcal{L} = -\frac{1}{4}(\partial_\mu A_\nu - \partial_\nu A_\mu)^2 + \bar{\psi}(i\not{\partial} - e\not{A} - m)\psi, \quad (1)$$

where  $A_\mu$  is the Lorentz vector that represents the photon field and  $\psi$  is the spinor of a fermion with electric charge  $e$ . In  $D = 3 + 1$ ,  $\psi$  is required to have four components. Though that is not necessary in  $D = 2 + 1$ , we may nevertheless choose so.

In radial gauge, the flux tube configuration reads

$$A_0 = 0, \quad \vec{A} = \frac{F}{2\pi r} f(r) \hat{e}_\varphi, \quad B(r) = \frac{F}{2\pi r} \frac{df(r)}{dr}, \quad (2)$$

where  $B$  denotes the magnetic field. For a Gaussian flux tube, we thus find

$$f_G(r) = 1 - e^{-r^2/w^2}, \quad B_G(r) = B_G(0) e^{-r^2/w^2}, \quad (3)$$

which implies that the net flux  $F_G = \pi w^2 B_G(0)$  and the classical energy

$$E_{\text{cl}} = \frac{1}{2} \int d^2r B^2(\vec{r}) \quad (4)$$

in  $D = 2 + 1$ . For  $D = 3 + 1$ , the identical expression gives the classical energy per unit length of the flux tube. We adopt the one-loop approximation wherein the background fields consist only of gauge fields; so do the external lines of the Feynman diagrams. Thus, we only consider fermions loops in the one-loop approximation and the only relevant counterterm Lagrangian is

$$\mathcal{L}_{\text{ct}} = -\frac{C^{(D)}}{4} F_{\mu\nu} F^{\mu\nu}. \quad (5)$$

It is natural to impose the renormalization condition that at zero momentum transfer the photon wavefunction is not altered by quantum effects. This yields  $C^{(3)} = -\frac{e^2}{6\pi m}$  and  $C^{(4-\epsilon)} = -\frac{e^2}{12\pi^2} \left( \frac{2}{\epsilon} - \gamma + \ln \frac{4\pi}{m^2} \right)$  in  $D = 2 + 1$  and  $D = 3 + 1 - \epsilon$  dimensions, respectively. Note that the renormalization coefficient is finite in  $D = 2 + 1$  while we have employed dimensional regularization in  $D = 3 + 1$ . The corresponding counterterm energy (resp. energy per unit length) is

$$E_{\text{ct}}^{(D)} = \frac{C^{(D)}}{2} \int d^2x B^2. \quad (6)$$

### 3. Fermion determinant

We obtain the vacuum polarization energy from the fermion loop by computing the functional determinants

$$\begin{aligned} E_{\text{vac}}^{(3)} &= \lim_{T \rightarrow \infty} \frac{i}{T} [\ln \text{Det}(i\hat{D} - e\hat{A} - m) - \ln \text{Det}(i\hat{D} - m)] + E_{\text{ct}}^{(3)}, \\ E_{\text{vac}}^{(4)} &= \lim_{T, L_z \rightarrow \infty} \frac{i}{TL_z} [\ln \text{Det}(i\hat{D} - e\hat{A} - m) - \ln \text{Det}(i\hat{D} - m)] + E_{\text{ct}}^{(4)}. \end{aligned} \quad (7)$$

Again, we consider the energy per unit length of the flux tube. Note that by inclusion of the counterterm contribution the above expressions are ultraviolet finite. In order to perform this computation, we have to consider the non-trivial (static) background field  $A_\mu(\vec{x}) \neq 0$  of the flux tube, cf equation (3) in the Dirac equation:

$$[\vec{\alpha} \cdot (\vec{p} + \vec{A}(\vec{x})) + \beta m]\Psi = \omega\Psi. \quad (8)$$

The interaction induces a potential for the fluctuating fermions' fields with two essential properties. First, bound states with energies  $\omega_j$  may emerge. In magnitude, these energies are smaller than the fermion mass  $m$ .<sup>1</sup> Second, the continuum levels  $\omega = \pm\sqrt{k^2 + m^2}$  acquire a non-zero phase shift,  $\delta_\ell(k)$ , which translates into a modification of the level density,  $\Delta\rho(k) = \frac{1}{\pi} \sum_{\ell, \pm} \frac{d}{dk} [\delta_\ell(k)]$ . Here  $\ell$  is the orbital angular momentum quantum number according to which the modes decouple and  $k$  is the linear momentum of the fluctuating field. We then find the vacuum polarization energy

$$\begin{aligned} E_\delta^{(3)} &= -\frac{1}{2} \sum_j (|\omega_j| - m) + \frac{1}{2\pi} \int_0^\infty dk \frac{k}{\sqrt{k^2 + m^2}} \sum_\ell \bar{\delta}_\ell(k), \\ E_\delta^{(4)} &= -\frac{1}{8\pi} \sum_j \left( \omega_j^2 \ln \frac{\omega_j^2}{m^2} + m^2 - \omega_j^2 \right) - \frac{1}{4\pi^2} \int_0^\infty dk k \ln \frac{k^2 + m^2}{m^2} \sum_\ell \bar{\delta}_\ell(k), \end{aligned} \quad (9)$$

$$\bar{\delta}_\ell(k) = \delta_\ell(k) - \delta_\ell^{(1)}(k) - \delta_\ell^{(2)}(k).$$

In  $D = 3 + 1$ , the energy per unit length is obtained from the interface formalism of [17]. It is important to stress that we have subtracted the first two orders of the Born series from the integrand to render the integrals finite. We will add back these pieces in the form of Feynman diagrams,  $E_{\text{FD}}^{(D)}$ . The identity between the Born and the Feynman diagram contributions at a prescribed order has been verified within dimensional regularization [18] and tested numerically, see e.g. appendix B of [19]. This procedure has the advantage that the renormalization conditions from the perturbative sector of the theory may be adopted [20]. To this end, the renormalized vacuum polarization energy reads

$$E_{\text{vac}}^{(D)} = E_\delta^{(D)} + E_{\text{FD}}^{(D)} + E_{\text{ct}}^{(D)}. \quad (10)$$

### 4. Embedding

Configurations like equation (3) with non-zero net flux induce potentials that behave like  $V_{\text{eff}}(r) \sim 1/r^2$  as  $r \rightarrow \infty$  in the second-order differential equations for the radial functions from which we extract the bound-state energies and phase shifts. This behaviour violates standard conditions necessary to deduce the analytic structure of scattering data in the complex momentum plane. As a direct consequence, we observe that the phase shifts are discontinuous

<sup>1</sup> For the flux tube configurations only threshold states with  $|\omega_j| = m$  occur. The configurations that we consider in section 4 do not have any bound states.

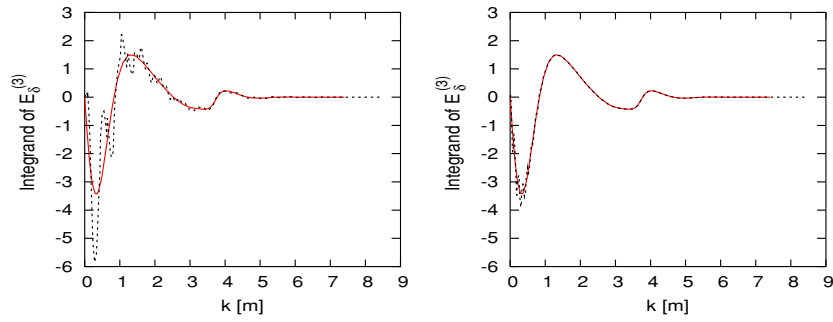


**Figure 1.** The integrands of  $E_\delta^{(3)}$ , equation (9), with (black dashed lines) and without (red full lines) return fluxes for  $R = 6/m$  (left panel) and  $R = 26/m$  (right panel).

as  $k \rightarrow 0$  and Levinson's theorem cannot be employed to reliably predict the number of bound states. Though this is not a principle obstacle because we have other means to find the bound states and any singularity at  $k = 0$  is integrable in equation (9), it puts doubts on the use of scattering data for this computation. The analytic structure is furthermore mandatory to relate the matrix element of the energy momentum tensor to formulae like equations (9) and (10) that underlie our computation of the renormalized vacuum polarization energy. At the same time, we observe that configurations with zero net flux are *unrealistic*. This becomes obvious from the Bianchi identity:

$$\epsilon^{\alpha\beta\mu\nu}\partial_\beta F_{\mu\nu} = 0. \quad (11)$$

In  $D = 3 + 1$ , this identity comprises the well-known Maxwell equation  $\vec{\partial} \cdot \vec{B}(\vec{x}) = 0$  stating that magnetic field lines must be closed or extend to spatial infinity outside the region of interest. The latter scenario is not adequate for the study of the vacuum energy which requires to integrate over full space. In  $D = 2 + 1$ , the Bianchi identity becomes  $\frac{\partial B}{\partial t} = -\partial_x E_y + \partial_y E_x$ . This implies that it is impossible to create (static) net flux configurations from zero flux. This may cause inconsistencies as we want to compare energies of configurations with and without fluxes. We therefore superimpose a *return flux* configuration according to

$$B_R(r) = -\frac{16F_G}{\pi R^2(1 + 256(r^2/R^2 - 1)^2)(\pi/2 + \arctan(16))}, \quad (12)$$

$$B_0(r) = B_G(r) + B_R(r).$$

In the following, we will refer to this configuration as the zero net flux configuration. It is straightforward to verify that  $\lim_{R \rightarrow \infty} E_{\text{cl}}[B_0] = E_{\text{cl}}[B_G]$  and  $\lim_{R \rightarrow \infty} E_{\text{FD}}[B_0] = E_{\text{FD}}[B_G]$ . That is, the return flux does not contribute to the classical and counterterm energies as the position  $R$  of the return flux is sent to spatial infinity. The crucial question obviously is about the behaviour of  $E_{\text{vac}}[B_0]$  as  $R \rightarrow \infty$ . To see what happens, we compare the integrands of  $E_\delta^{(3)}$  for configurations with and without fluxes for two values of  $R$  in figure 1. The integrand corresponding to  $B_0$  oscillates around that corresponding to  $B_G$  and these oscillations diminish as  $R$  increases. This indicates that indeed  $\lim_{R \rightarrow \infty} E_{\text{vac}}[B_0] = E_{\text{vac}}[B_G]$ . In order to unambiguously decide on that question, we have to consider the energy density. This will allow us to distinguish between the contributions from the centre flux tube and the return flux.

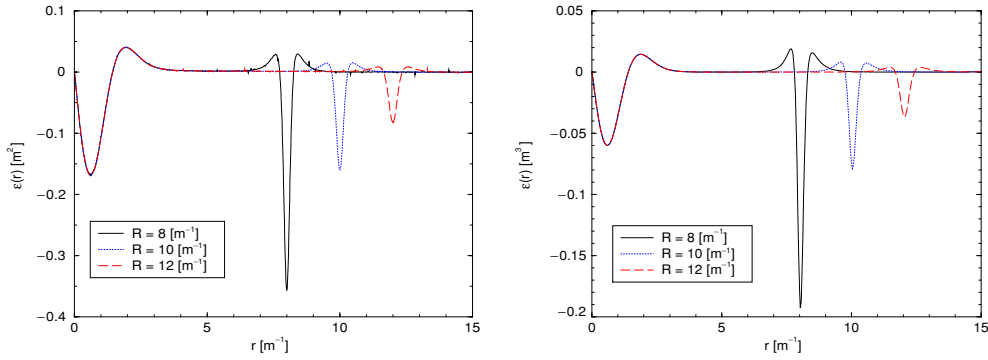


**Figure 2.** The left panel shows the energy density  $\epsilon(r)$  for various values of the return flux position  $R$  in  $D = 2 + 1$ . The right panel is the analogue for the energy density per unit length of the vortex in  $D = 3 + 1$ .

## 5. Energy density

As motivated above, we consider the vacuum polarization energy density

$$\epsilon(r) = 2\pi r \langle T_{00} \rangle \quad (13)$$

to decide whether or not a vacuum polarization energy can be attributed to a single flux tube. Here  $\langle T_{00} \rangle$  denotes a specific matrix element of the energy momentum tensor  $T_{\mu\nu}$  in the background of the zero net flux configuration. As for the total energy the energy density is computed from three entries,

$$\epsilon(r) = \epsilon_\delta(r) + \epsilon_{\text{FD}}(r) + \epsilon_{\text{ct}}(r), \quad (14)$$

the contribution from scattering data,  $\epsilon_\delta(r)$ , with appropriate Born terms subtracted to render the momentum integrals finite, the Feynman diagram contribution,  $\epsilon_{\text{FD}}(r)$ , as the Born subtractions must be added back and the counterterm contribution from  $\mathcal{L}_{\text{ct}}$ , equation (5). For the details on this computation we refer to [1], in particular for the discussion on how the counterterm contribution cancels the UV divergences without the need for additional surface counterterms. Of course, a general consistency condition is that equation (10) is obtained from the spatial integral  $\int_0^\infty dr \epsilon(r)$ . This requires to consider zero net flux configurations because only then the analytic properties of the scattering data are guaranteed that underlie the proof of that identity, cf [21].

In figure 2, we display the energy density as a function of the return flux position,  $R$ . A number of conclusions can be drawn from these numerical studies: (1) the energy density in central region of small  $r$  is independent of  $R$ ; (2) the integrated density from that region gives  $\lim_{R \rightarrow \infty} \int_0^{R/2} dr \epsilon(r) = E_{\text{vac}}[B_G]$ ; (3) the energy from the return flux diminishes as its position is sent to infinity, i.e.  $\lim_{R \rightarrow \infty} \int_{R/2}^\infty dr \epsilon(r) = 0$ . Altogether this is good news as it clearly confirms the naïve method that only considers a single central flux tube. The discontinuities in the phase shifts at  $k = 0$  do not propagate to the vacuum polarization energy.

## 6. Approximation schemes for $E_{\text{vac}}[B_G]$

Having established a reliable method for the computation of the vacuum polarization energies of flux tubes provides a good opportunity to employ this method to judge approximation

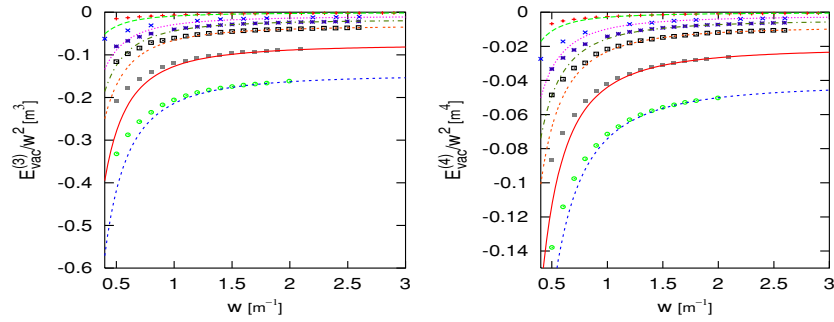


**Figure 3.** Renormalized one-loop energies in  $D = 2 + 1$  (left panel) and  $D = 3 + 1$  (right panel), for fixed values of the magnetic field at the origin, as a function of the width of the Gaussian flux tube. The lines correspond to the derivative expansion to second order [5]. The dots, circles, etc represent the exact results for  $E_{\text{vac}}$ . From top to bottom,  $eB_G(0)/m^2 = 1.1, 2, 2.5, 3, 4, 5$ .

schemes. Most popular are the derivative and perturbative expansion schemes. In both cases, we will study the dependence of the vacuum polarization energy on the width  $w$ , introduced in equation (3). It is important to consider variations of the background field that are consistent with the respective scheme. For example, for the derivative expansion to be appropriate we require configurations that vary slowly but keep the amplitude  $B_G(0)$  fixed. In contrast, for the perturbative expansion we wish to consider different amplitudes and thus keep the magnetic flux  $F_G$  fixed as we change  $w$ . The results for the derivative expansion are shown in figure 3. In both cases,  $D = 2 + 1$  and  $D = 3 + 1$ , we find good agreement between the exact result and the leading contributions in the derivative expansion, even though the derivative expansion is known to be an asymptotic expansion and hence does not converge when summed to all orders [6]. In the perturbative expansion, we evaluate the leading Feynman diagram,

$$E_{\text{FD}}^{(D)} = \frac{8\pi \mathcal{F}^2}{(4\pi)^{D/2}} \int_0^\infty dp \left[ \int_0^\infty dr \frac{df(r)}{dr} J_0(pr) \right]^2 \int_0^1 dx \frac{x(1-x)p\Gamma(2-D/2)}{[m^2 + p^2x(1-x)]^{2-D/2}}, \quad (15)$$

in  $D = 2 + 1$  and  $D = 3 + 1$  dimensions with the effective expansion parameter  $\mathcal{F} = \frac{e}{2\pi} F_G$ . The UV divergence has not yet been removed from the diagram, equation (15), and the counterterm part has to be added. This is illuminating especially for  $D = 2 + 1$  because with our renormalization condition it changes the leading behaviour from  $\mathcal{F}/w^2$  to  $\mathcal{F}^2/w^4$ . Stated otherwise, renormalization is essential even for finite quantities. The change in this leading behaviour is crucial to obtain agreement between the exact results and the perturbative expansion, both in  $D = 2 + 1$  and in  $D = 3 + 1$ , cf figure 4.

Obviously, the approximation schemes work well for the  $D = 2 + 1$  and  $D = 3 + 1$  cases. Furthermore, the vacuum polarization energies are negative and decrease with the width of the background flux tube for both cases. Also the energy densities (per unit length in  $D = 3 + 1$ ) are similar in structure as can, e.g., be seen from figure 2. As discussed above, to obtain these similarities it has been crucial to impose *identical* renormalization conditions. Having done so, it is to be expected that the simpler  $D = 2 + 1$  case can be utilized to gain information about vacuum polarization energies of vortex configurations in more complicated  $D = 3 + 1$  problems [16].

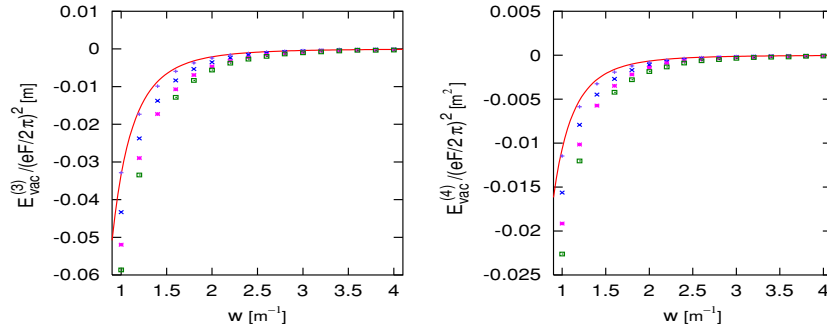


**Figure 4.** Renormalized fermion vacuum polarization energy in units of  $\mathcal{F}^2$  as a function of the width, for various fixed values of the flux  $\mathcal{F}$  (2.5, 4.5, 6.5, 8.5 from top to bottom) in the Gaussian flux tube. The full line represents the leading perturbation expansion contribution. The left panel is for  $D = 2 + 1$  and the right panel for  $D = 3 + 1$ .

## 7. Conclusions

In this paper, I have reported on computations that we have performed for one-loop energies and energy densities of electromagnetic flux tubes in three and four spacetime dimensions. In general, this vacuum polarization energy contains ultraviolet divergences and an important feature of our approach is that it allows us to impose the standard renormalization conditions of perturbative quantum electrodynamics. Even though the calculation in three spacetime dimensions does not suffer from such divergences, a meaningful comparison between three and four dimensions can only be made when identical renormalization conditions are imposed. The use of scattering data to compute the vacuum polarization energy of an individual flux tube leads to subtleties arising from the long-range potential associated with the flux tube background, which does not satisfy the standard conditions of scattering theory. Consequently, the scattering data do not necessarily have the standard analytic properties required to relate the vacuum polarization energy to scattering data. We have therefore considered field configurations in which the flux tube is embedded with a well-separated return flux so that the total flux vanishes. We have constructed a limiting procedure in which this return flux does not contribute to the energy, enabling us to compute the energy of an isolated flux tube.

We do not find qualitative differences between three and four dimensions for either the energy or the energy density, once identical renormalization conditions have been imposed. However, we stress that renormalization in the case of three dimensions proved essential to this result because the (finite) counterterm contribution turned out to be large, thus causing sizable cancellations in the final result.

This study gives an initial step towards understanding flux tubes and vortices in more complicated theories. In particular, the similarities between the three- and four-dimensional cases can be used to determine whether quantum corrections stabilize the classically unstable strings in the standard model [16].

## Acknowledgments

In this paper, I have presented results that originated from a collaboration with N Graham, V Khemani, M Quandt and O Schröder. I highly appreciate their contribution. Also support from the DFG under contract We-1254/10-1 is acknowledged.



## References

- [1] Graham N, Khemani V, Quandt M, Schroeder O and Weigel H 2005 *Nucl. Phys. B* **707** 233
- [2] Aharonov Y and Casher A 1979 *Phys. Rev. A* **19** 2461
- [3] Alford M and Wilczek F 1989 *Phys. Rev. Lett.* **62** 1071
- [4] Redlich A N 1984 *Phys. Rev. D* **29** 2366
- [5] Cangemi D, d'Hoker E and Dunne G V 1995 *Phys. Rev. D* **51** 2513  
Gusynin V P and Shovkovy I A 1999 *J. Math. Phys.* **40** 5406  
Lee H W, Pac P Y and Shin H K 1989 *Phys. Rev. D* **40** 4202
- [6] Dunne G V and Hall T M 1998 *Phys. Lett. B* **419** 322  
Dunne G V and Hall T M 1999 *Phys. Rev. D* **60** 065002
- [7] Blankenbecler R and Boyanovsky D 1986 *Phys. Rev. D* **34** 612
- [8] Kiskis J 1977 *Phys. Rev. D* **15** 2329
- [9] Niemi A J and Semenoff G W 1983 *Phys. Rev. Lett.* **51** 2077
- [10] Bordag M and Kirsten K 1999 *Phys. Rev. D* **60** 105019
- [11] Langfeld K, Moyaerts L and Gies H 2002 *Nucl. Phys. B* **646** 158
- [12] Achucarro A and Vachaspati T 2000 *Phys. Rep.* **327** 347
- [13] Vachaspati T 1992 *Phys. Rev. Lett.* **68** 1977
- [14] Farhi E, Graham N, Jaffe R L and Weigel H 2000 *Nucl. Phys. B* **585** 443
- [15] Newton R G 1982 *Scattering Theory of Waves and Particles* (New York: Springer)  
Chadan K and Sabatier P C 1989 *Inverse Problems in Quantum Scattering Theory* (New York: Springer)
- [16] Schroeder O 2006 *J. Phys. A: Math. Gen.* **39** 6733 (Preprint [hep-th/0601196](https://arxiv.org/abs/hep-th/0601196))  
Graham N, Khemani V, Quandt M, Schroeder O and Weigel H in preparation
- [17] Graham N, Jaffe R L, Quandt M and Weigel H 2001 *Phys. Rev. Lett.* **87** 131601
- [18] Farhi E, Graham N, Jaffe R L and Weigel H 2001 *Nucl. Phys. B* **595** 536
- [19] Farhi E, Graham N, Jaffe R L and Weigel H 2002 *Nucl. Phys. B* **630** 241
- [20] Graham N, Jaffe R L and Weigel H 2002 *Int. J. Mod. Phys. A* **17** 846
- [21] Graham N, Jaffe R L, Khemani V, Quandt M, Scandurra M and Weigel H 2002 *Nucl. Phys. B* **645** 49